

Estimating changes in heat energy stored within a column of wetland surface water and factors controlling their importance in the surface energy budget

W. Barclay Shoemaker

Center for Water and Restoration Studies, Florida Integrated Science Center, U.S. Geological Survey, Miami, Florida, USA

David M. Sumner

Center for Aquatic Resource Studies, Florida Integrated Science Center, U.S. Geological Survey, Altamonte Springs, Florida, USA

Adrian Castillo

Center for Water and Restoration Studies, Florida Integrated Science Center, U.S. Geological Survey, Miami, Florida, USA

Received 14 February 2005; revised 12 July 2005; accepted 25 July 2005; published 21 October 2005.

[1] Changes in heat energy stored within a column of wetland surface water can be a considerable component of the surface energy budget, an attribute that is demonstrated by comparing changes in stored heat energy to net radiation at seven sites in the wetland areas of southern Florida, including the Everglades. The magnitude of changes in stored heat energy approached the magnitude of net radiation more often during the winter dry season than during the summer wet season. Furthermore, the magnitude of changes in stored heat energy in wetland surface water generally decreased as surface energy budgets were upscaled temporally. A new method was developed to estimate changes in stored heat energy that overcomes an important data limitation, namely, the limited spatial and temporal availability of water temperature measurements. The new method is instead based on readily available air temperature measurements and relies on the convolution of air temperature changes with a regression-defined transfer function to estimate changes in water temperature. The convolution-computed water temperature changes are used with water depths and heat capacity to estimate changes in stored heat energy within the Everglades wetland areas. These results likely can be adapted to other humid subtropical wetlands characterized by open water, saw grass, and rush vegetation type communities.

Citation: Shoemaker, W. B., D. M. Sumner, and A. Castillo (2005), Estimating changes in heat energy stored within a column of wetland surface water and factors controlling their importance in the surface energy budget, *Water Resour. Res.*, *41*, W10411, doi:10.1029/2005WR004037.

1. Introduction

[2] Suitable spatial and temporal definition of changes in heat energy stored in a column of wetland surface water are frequently needed to make local and regional energy budget estimates of latent heat fluxes; that is, the energy equivalent of evapotranspiration. Uncertainties in the characterization of surface energy fluxes limit the reliability of hydrologic analyses, and handicap efforts to manage water resources. The purposes of this paper are to (1) identify when and where changes in stored heat energy in wetland surface water are a considerable component of the surface energy budget and (2) introduce new equations for computing changes in wetland stored heat energy that rely on measured changes in air temperature rather than measured changes in water temperature. Reliance on air temperature instead of water temperature was considered desirable because air temperature data are more readily available. Additionally,

air temperature monitoring is less expensive and less labor intensive than water temperature monitoring. The new equations for computing changes in heat energy stored in wetland surface water are applied in a case study of the Everglades areas of southern Florida (Figure 1).

[3] A simplified surface energy budget for wetlands takes the form (Figure 2)

$$R_n - (W + G_{veg}) = \lambda E + H \quad (1)$$

where R_n is net radiation, W is changes in heat energy stored in wetland surface water, G_{veg} is biomass storage (heat energy stored in the vegetation), λE is the latent heat flux, and H is the sensible heat flux. The units for these surface energy fluxes are watts per square meter ($W\ m^{-2}$). The terms on the left side of the energy budget equation are commonly called the available energy (Ae) for evapotranspiration because this energy is partitioned between sensible heat (H) and latent heat (λE). Typically, R_n is the dominant component of a surface energy budget; however, this does

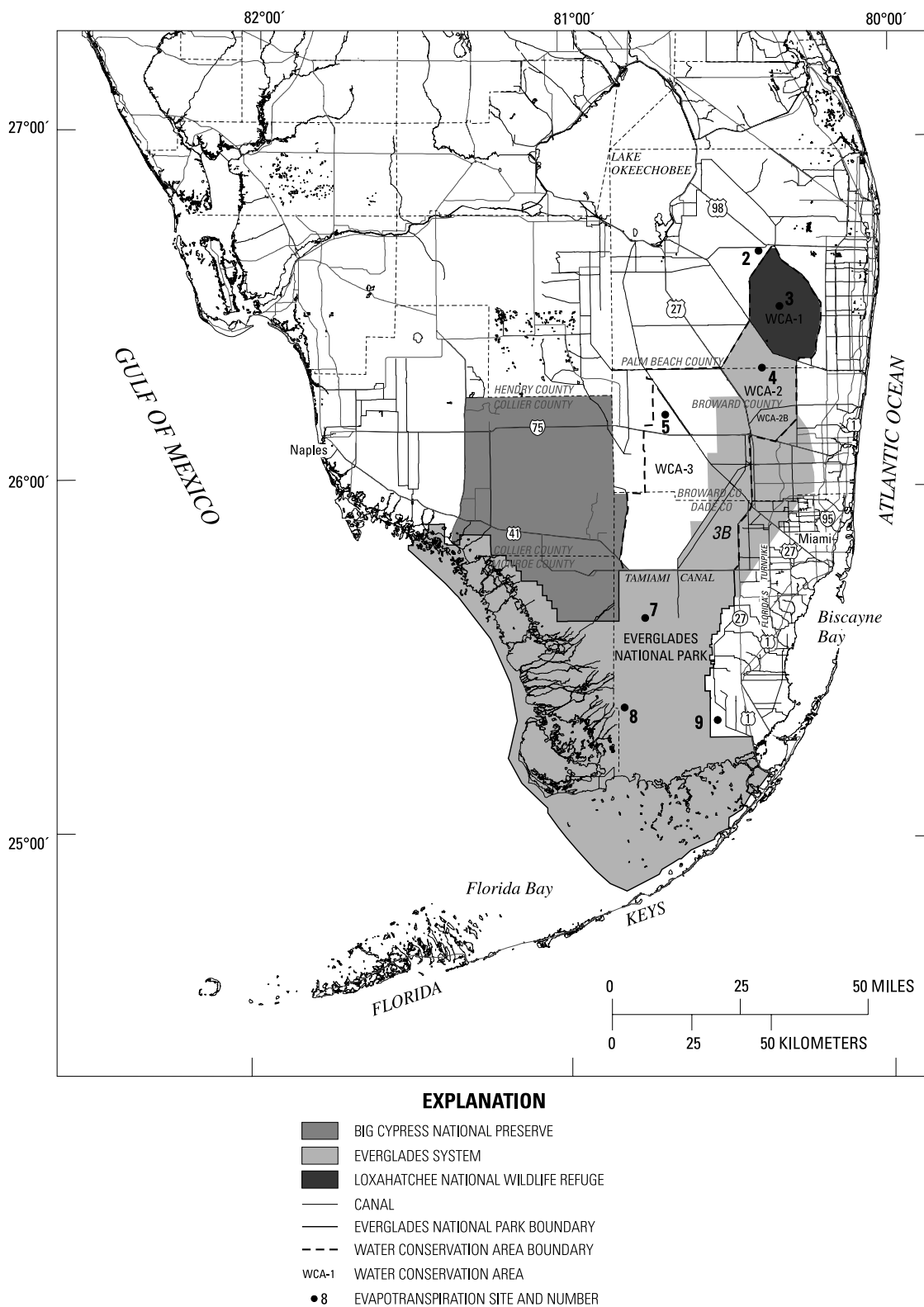
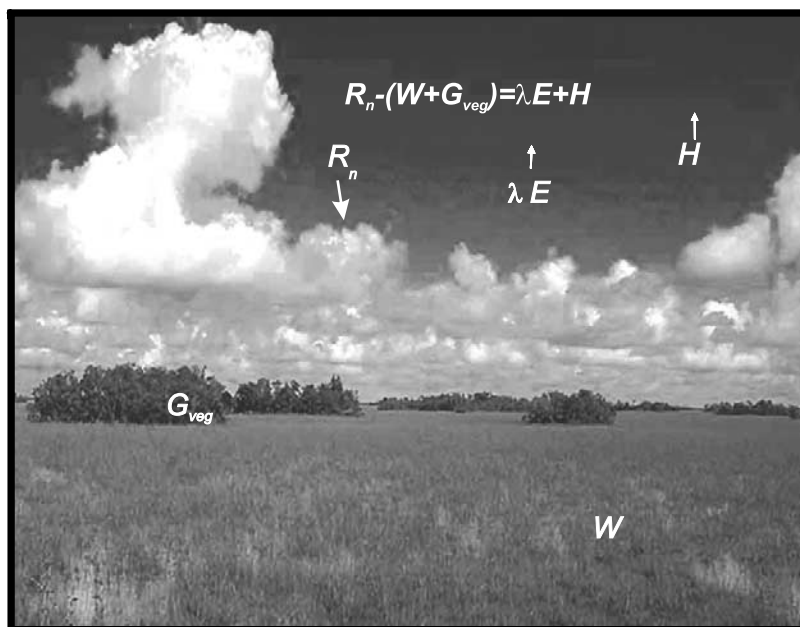


Figure 1. Location of study sites in the wetland areas of southern Florida. Modified from Lietz [2000].

not hold true universally because W can be considerable at locations with surface water. In fact, W sometimes can be the dominant component of a surface energy budget.

[4] Previous studies have investigated surface energy fluxes using land-based hydrometeorological methods [Brutsaert, 1982; Monteith and Unsworth, 1990; Abteu

and Obeysekera, 1995; Bidlake et al., 1996; Campbell and Norman, 1998; German, 2000; Lott and Hunt, 2001; Sumner, 2001; Jacobs and Satti, 2001; Wilson et al., 2002; Small and Kurc, 2003] and satellite-based methods [Anderson et al., 1997; Norman et al., 2003; Liu et al., 2003; Bastiaanssen et al., 2002; Islam et al., 2002].



EXPLANATION

- R_n Net radiation
- W Stored-heat energy in wetland surface water
- G Biomass storage (heat energy stored in the vegetation)
- λE Latent heat flux
- H Sensible heat flux

Figure 2. Simplified surface energy budget for the Everglades.

Because a change in surface water temperature reflects a change in stored heat energy, previous studies of surface water temperature are considered relevant, including those of equilibrium surface water temperature [Edinger *et al.*, 1968; Bogan *et al.*, 2003] and heat exchange at the air-water interface [Mohseni *et al.*, 1998]. The latter studies, however, differ from the analysis described herein because they focus on absolute water temperatures rather than changes in water temperature. For example, Bogan *et al.* [2003] developed relations between mean weekly equilibrium stream temperature and mean weekly stream temperature, and Mohseni *et al.* [1998] examined the relation between mean weekly air and stream temperatures. Edinger *et al.* [1968] introduced the concept of equilibrium water temperature, defining it as

the water temperature at which the sum of the heat fluxes through the surface water is zero.

2. Data Compilation and Equation Development

[5] New equations developed for estimating changes in heat energy stored in a column of wetland surface water are presented. Existing hydrometeorological data [German, 2000] in the Everglades wetland areas of southern Florida were compiled before these equations were developed.

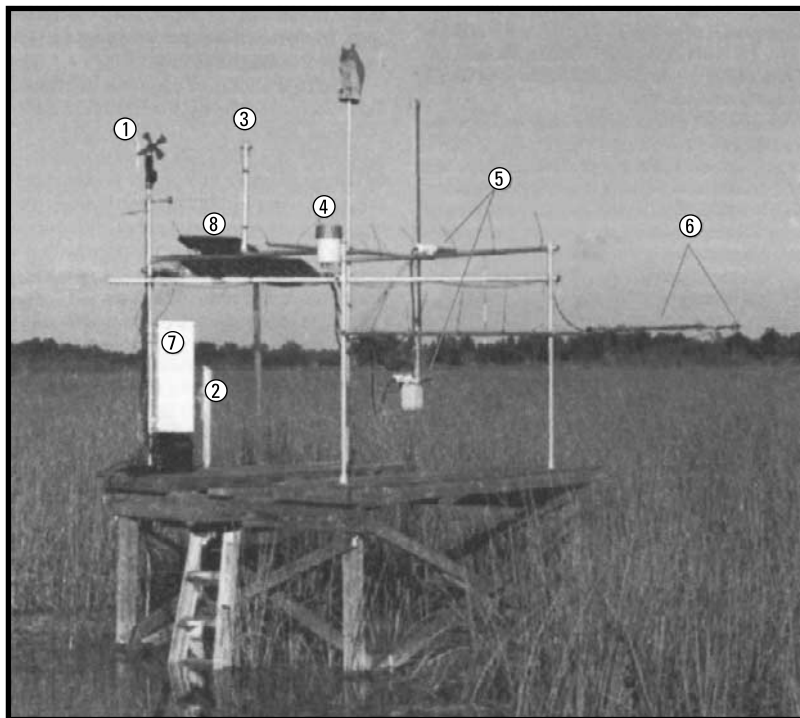
2.1. Data Compilation

[6] The hydrometeorological data compiled for this analysis were taken from German [2000] (Figure 1 and

Table 1. Site Locations and Characteristics in the Wetland Areas of Southern Florida^a

Site	Latitude	Longitude	Approximate Height Above Land Surface of Air Temperature Sensor, m	Community	Comments
2	26°37'40"	80°26'12"	1.5	open water	always wet; lily pads at times
3	26°31'20"	80°20'11"	1.4	open water	flow regulation
4	26°18'55"	80°22'57"	3.0	dense saw grass	dry part of some years
5	26°15'30"	80°44'17"	2.5	medium saw grass	dry part of some years
7	25°36'59"	80°42'08"	2.3	sparse saw grass	never dry
8	25°21'11"	80°38'02"	1.2	sparse rushes	dry part of each year
9	25°21'35"	80°31'46"	1.6	sparse saw grass	dry part of each year

^aLocations are shown in Figure 1.



EXPLANATION

1. WIND SPEED AND DIRECTION
2. STILLING WELL FOR WATER-LEVEL MEASUREMENT
3. PYRANOMETER
4. RAIN GAGE
5. AIR TEMPERATURE AND RELATIVE HUMIDITY SENSOR
6. NET RADIOMETERS
7. DATA LOGGER AND PHONE
8. SOLAR PANEL

Figure 3. Typical data collection site. From *German* [2000].

Table 1), who estimated evapotranspiration in the Everglades using a Bowen ratio approach [Bowen, 1926]. Data collected at sites included the surface water depth, rainfall, wind speed and direction, incoming solar radiation, net radiation, soil heat flux, air temperature, relative humidity, vapor pressure gradient, air temperature gradient, and water temperature at both the water surface and at depth. An example of a typical data collection site is shown in Figure 3.

[7] At each site, sensor measurements were made every 30 s and averaged and stored on site at 15 or 30 min intervals [German, 2000]. Measurements were stored at 15 min intervals at sites 4–9. Thirty minute means or totals (for rainfall) were computed for sites 4–9 so that analysis and equations could be applied at each location using data with a consistent time step. Data used most frequently in this paper are measurements of air and surface water temperature, and surface water depth. German [2000] measured surface water temperature (1) directly below the water surface, and (2) at depth near the land-water interface adjacent to decaying peat and vegetation at the bottom of the surface water column. The height above land surface where air temperature was

measured ranged from about 1 to 4 m (Table 1), and depended on the vegetation height.

[8] German [2000] describes in detail (1) the criteria for selecting monitoring sites, (2) data processing and screening, and (3) site maintenance; these procedures are summarized here. Factors considered in site selection included plant community, duration of water inundation, security and logistics. Each site was located at the center of a circle of relatively uniform vegetative cover with a radius of at least 100 times the height of the air temperature/relative humidity sensor. Data processing included screening tests based on range limits and visual inspections to eliminate data collected by sensors that were clearly malfunctioning. Sites were visited every 4 to 6 weeks for inspection and maintenance. It is important to note the accuracy of air and water temperature measurements used in this study. Accuracy of these measurements may be about $\pm 0.4\%$ of the reading (Omega Engineering Inc., oral communication, 2005). The mean temperatures measured at all nine sites were about 23.3° and 25.1°C , respectively, for air and water [German, 2000] which translates into an average error of about $\pm 0.1^\circ\text{C}$. An error of $\pm 0.2^\circ\text{C}$ is possible for air and water

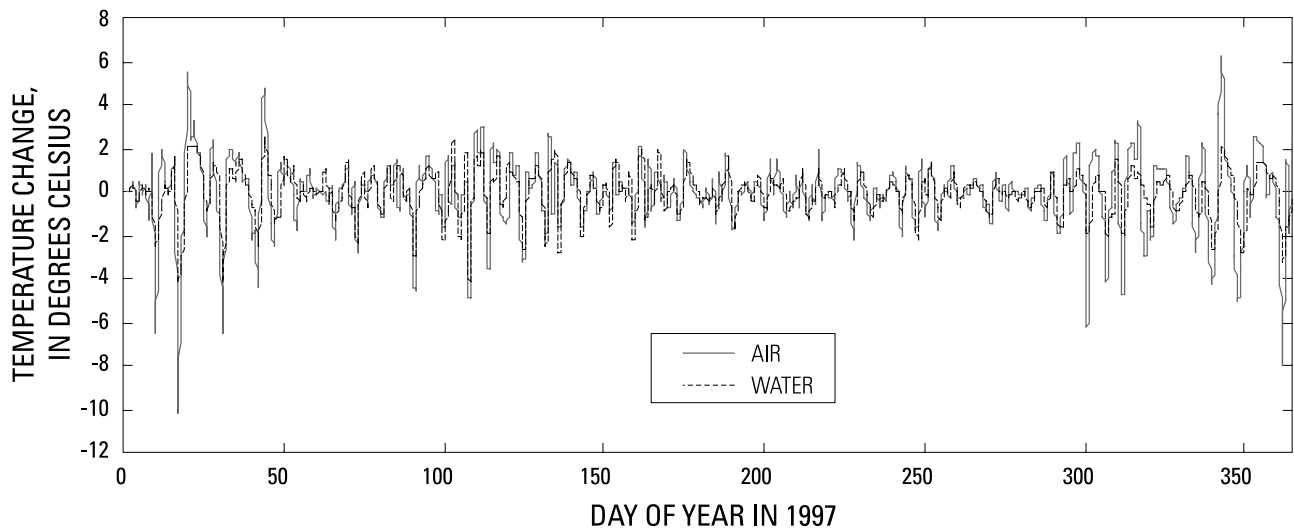


Figure 4. Changes in mean daily and vertical water and air temperatures at site 3 in the Everglades during 1997. Site location is shown in Figure 1.

temperature changes, since these are the difference between two consecutive readings.

2.2. Equation Development

[9] Several equations were considered to estimate changes in stored heat energy in a column of wetland surface water. The goals were to (1) capture (reasonably well) the observed variability in stored heat energy changes at 30 min and daily time intervals, and (2) require only readily available data.

[10] Estimating stored heat energy changes at short time intervals (30 min and daily) was desirable because high-frequency estimates are needed to make local and regional energy budget estimates of evapotranspiration. For example, 30 min and daily fluxes of stored heat energy can be used to estimate evapotranspiration with the Priestley-Taylor [Priestley and Taylor, 1972] and Penman [1948] equations. Also, high-frequency results can be temporally up-scaled to fit the needs of most evapotranspiration estimators. For example, 30 min fluxes of stored heat energy can be up-scaled to weekly and monthly values for energy budget based estimators of evapotranspiration.

[11] Ideally, stored heat energy is calculated from changes in the vertically averaged water column temperature measured by thermistor or thermocouple strings. Unfortunately, historical water temperature data are limited. Historical air temperature data, however, are readily available and, for shallow layers of surface water, air temperature changes are the primary driver of water temperature changes. For example, air temperature changes explain most of the variability in water temperature changes in Everglades wetland areas. The similarity of changes in mean daily air and surface water temperatures at site 3 in 1997 demonstrates this point (Figure 4). These temperature changes were computed as the difference between two consecutive mean vertical and daily surface water temperatures. Although air temperature changes seem to explain most of the variability in water temperature changes, some differences are apparent (Figure 4). The differences could be caused by heat

exchange processes other than air temperature affecting water temperature, including water management activities, evaporative cooling, rainfall, and perhaps surface water and groundwater interactions.

[12] The goal of capturing the variability of changes in stored heat energy at short-time intervals (less than 1 hour) presented additional challenges, particularly the ability to account for the thermal memory of the wetland surface water. Thermal memory is a length of time that an individual air temperature change will impact future water temperature changes. Air temperature changes within the surface water's thermal memory are dampened, phase shifted, and superimposed to produce the current water temperature change (Figure 5). Air temperature changes that occurred more recently within the surface water's thermal memory impact the current water temperature change more strongly than air temperature changes that occurred later within the surface water's thermal memory. Notably, the concept of thermal memory differs from the concept of thermal inertia, which is the square root of the product of the media thermal conductivity, density and specific heat capacity. Thermal inertia is the ability of a material to conduct and store heat, whereas thermal memory only represents a length of time. Although not previously applied to heat exchange hydrologic problems, the general convolution integral can account for the thermal memory of surface water when computing changes in mean vertical surface water temperature.

2.2.1. Convolution Integral

[13] The convolution integral [Dodge, 1959; Besbes and DeMarsily, 1984; Morel-Seytoux, 1984; Wu et al., 1997; Weiler et al., 2003; Long and Putnam, 2004; O'Reilly, 2004] uses a time series forcing function and transfer function to calculate a time series response function. For this paper, the physics of heat energy exchange between the atmosphere and surface water is encapsulated as both a time-varying and nonlinear transfer function. The transfer function is time varying because the amount of heat energy exchanged between the atmosphere and surface water depends not only on the temperature gradient close the water surface, but also the surface-water depth, which can change within the

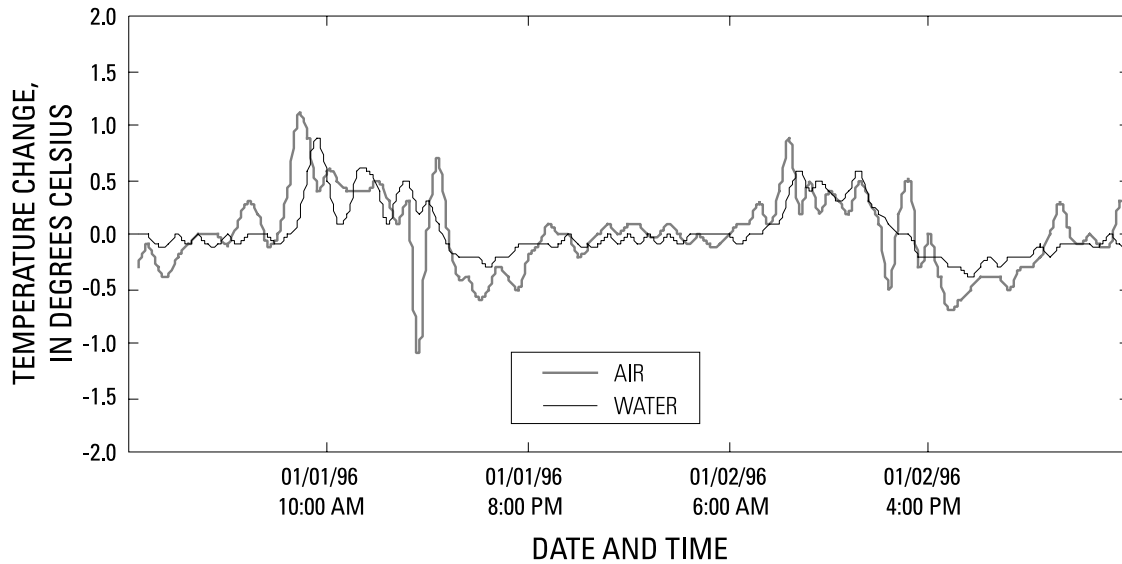


Figure 5. Changes in 30 min mean air and water temperature at site 3 in the Everglades. Site location is shown in Figure 1.

water's thermal memory. The nonlinearity of the transfer function is a consequence of its derivation from heat transfer equations, which will be discussed later.

[14] Numerous studies have used the convolution integrals. For example, *Besbes and DeMarsily* [1984] used the convolution of a time series of infiltrated water (forcing function) with a linear transfer function to compute a net recharge time series (response function) for an unconfined aquifer in northern France. *Long and Putnam* [2004] used the convolution of a time series of the stable isotope of oxygen ($\delta^{18}\text{O}$) for recharge water (forcing function) with a nonlinear transfer function (representing the effect of conduit and intermediate groundwater flow) to compute a time series of $\delta^{18}\text{O}$ (response function) at a discharge point. In this paper, the convolution integral is presented in a format similar to that of *Long and Putnam* [2004] and takes the form

$$y(t) = \int_0^t h(t-\tau)c(\tau)d\tau \quad (2)$$

where $y(t)$ is the computed time series of changes in mean vertical surface water temperature (the response function), $h(t-\tau)$ is the time-varying and nonlinear transfer function derived and described herein, $c(\tau)$ is the time series of measured changes in air temperature (the forcing function), and $d\tau$ is the derivative of time.

[15] Using the discrete form of the convolution integral, changes in the response function (water temperature) were computed as the linear superposition of a thermal memory of dampened and phase-shifted individual changes in the forcing function (air temperature). The discrete form of the convolution integral for this heat exchange problem is

$$y_i = \sum_{j=0}^{\text{IMEM}} h_{i-j}c_{i-j} \quad j = 0, 1, 2, \dots, \text{IMEM} \quad (3)$$

where y , h , and c are the discrete forms of the continuous functions in equation (2); i is the integer time step for computing changes in the response function (surface water temperature); and j is the integer time step discretizing the surface water's thermal memory. The variable $\text{IMEM} + 1$ is the number of historical time steps discretizing the surface water's thermal memory. Not present is an equation symbol for the water's thermal memory; instead, the thermal memory is the time length spanning the summation of the individual products of h and c from $j = 0$ to IMEM . Note that the transfer function, h_{i-j} , needs to be derived.

2.2.2. Transfer Function

[16] The transfer function describes the temporal response of the response function to a unit change in the forcing function and, as such, encapsulated the physics of heat exchange between the atmosphere and surface water. Assume that the derivative with respect to time of the difference between the equilibrium [*Edinger et al.*, 1968] and actual water temperatures is proportional to the difference between equilibrium and actual water temperatures and inversely proportional to surface water depth. The mathematical formula becomes

$$\frac{d(T_w^e - T_w)}{dt} = -k_{ex} \frac{(T_w^e - T_w)}{D}, \quad (4)$$

where T_w^e is equilibrium water temperature [T], T_w is actual water temperature [T], dt is the derivative of time [t], k_{ex} is the thermal exchange coefficient [Lt^{-1}], and D is the surface water depth [L]. The units [T], [t] and [L] represent the units of temperature, time and length, respectively. Equilibrium water temperature is defined as the temperature at which no net heat exchange occurs in the area of interest. This condition is met if the sum of various heat exchange processes, such as air temperature, sensible heat flux, solar radiation, and evaporative cooling totals zero. The k_{ex} variable is a proportionality constant that describes the rate at which water temperature responds to heat exchange processes [*Edinger et al.*, 1968]. In some cases treating k_{ex}

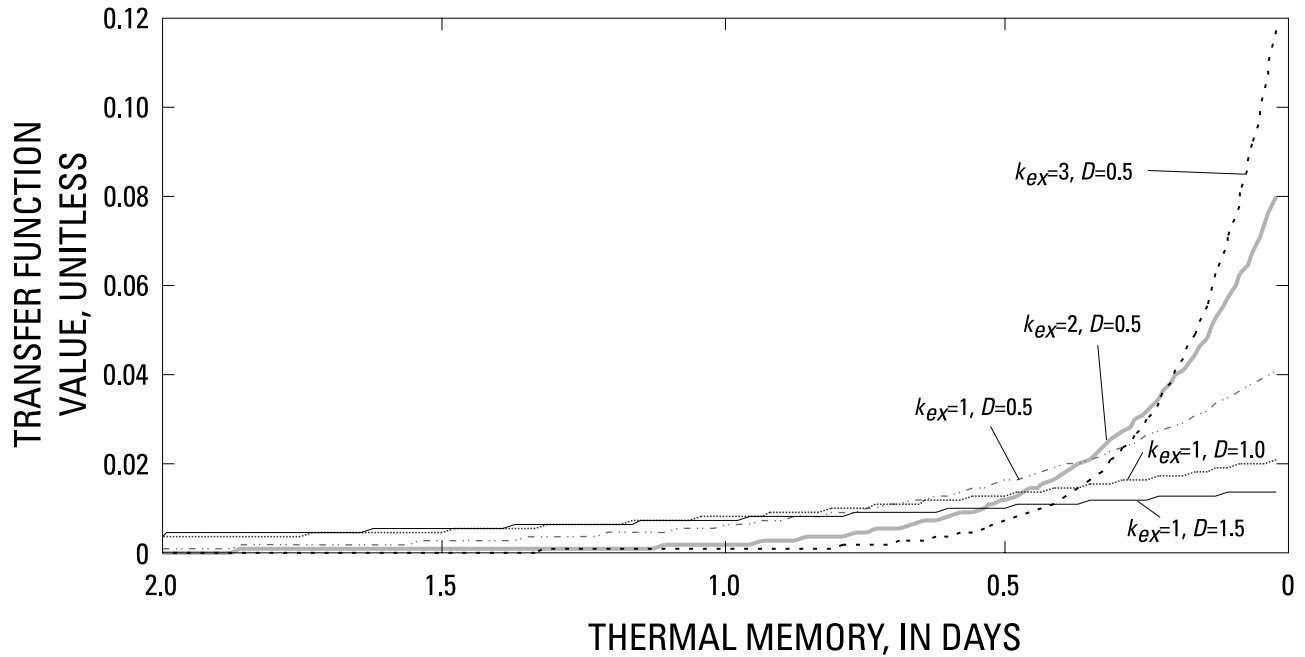


Figure 6. Transfer function for various values of the thermal exchange coefficient (k_{ex}) and surface water depth (D).

as a constant may oversimplify the actual system dynamics because k_{ex} likely depends on processes such as the temperature gradient near the water surface, local turbulence, and radiation.

[17] Solving the ordinary differential equation (4) (see Appendix A) yields

$$T_w = T_w^e - \Delta T_a e^{-\frac{k_{ex}}{D}t}, \quad (5)$$

where ΔT_a is the rate of change in air temperature [Tt-1]. The rate of change in water temperature with time is determined by differentiating equation (5) with respect to time, which results in

$$\frac{dT_w}{dt} = \Delta T_a \frac{k_{ex}}{D} e^{-\frac{k_{ex}}{D}t}. \quad (6)$$

The discrete form of this derivative introduces a coefficient, α (unitless), which relaxes the assumption that a specific air temperature change causes an equivalent water temperature change. The coefficient α represents the fraction of air temperature change that eventually causes an equivalent water temperature change, and is less than or equal to 1.0. This mathematical formula becomes

$$\frac{\Delta T_w}{\Delta t} = \alpha \Delta T_a \frac{k_{ex}}{D} e^{-\frac{k_{ex}}{D}t}. \quad (7)$$

Thus the transfer function takes the form

$$h_{i-j} = \frac{k_{ex}}{D_{i-j}} e^{-\frac{k_{ex}}{D_{i-j}}t}, \quad (8)$$

where t is the elapsed time within the surface water's thermal memory. The transfer function clearly is time

variant because of dependence on surface water depth, D_{i-j} , which changes within the thermal memory of the wetland surface water. The thermal exchange coefficient, k_{ex} , does not make the transfer function time variant because this coefficient is a regression-defined constant.

[18] The summation shown in equation (3) was carried out over an assumed finite thermal memory of the surface water. To avoid discretization errors, the transfer function was normalized by dividing by the total area under the discrete transfer function of finite memory. For various values of k_{ex} and D_{i-j} (Figure 6), a normalized form of the transfer function, equation (8), is indicative of exponential decay, suggesting air temperature changes that occurred more recently in the water's thermal memory have greater impact on current water temperature changes than air temperature changes that occurred later within the water's thermal memory. Increasing the thermal exchange coefficient, k_{ex} , reduces the impact of recent air temperature changes on the current water temperature change, and increases the impact of later air temperature changes on the current water temperature change. Likewise, an increased surface water depth, D_{i-j} , reduces the impact of recent air temperature changes on the current water temperature change but has little effect on the impact of later air temperature changes on the current water temperature change. The final discrete form of the transfer function and convolution integral, used to compute mean vertical water temperature changes, and ultimately, changes in heat energy stored in a column of wetland surface water, takes the form

$$\Delta T_{w_i} = \sum_{j=0}^{IMEM} \frac{k_{ex}}{D_{i-j}} e^{-\frac{k_{ex}}{D_{i-j}}t} \alpha \Delta T_{a_{i-j}} \quad j = 1, 2, 3, \dots, IMEM \quad (9)$$

[19] It is important to note that the distance between data collection locations may affect the accuracy of equation (9). For example, equation (9) is applied in the wetland areas of the Everglades (Figure 1), where air temperature measurements always were made less than 3 m away from the location where predicted mean vertical water temperature changes were desired. Using air temperatures measured several thousand meters away from the target location for predicting water temperature changes may increase the error statistics.

2.2.3. Parameter Estimation

[20] Regression was performed using UCODE [Poeter and Hill, 1998] to estimate parameter values for the transfer function that minimized the errors between mean vertical water temperature changes computed with the convolution integral and those measured in the field. Accurately computed water temperature changes are required to obtain accurate estimates of changes in heat energy stored in a column of wetland surface water. For example, an error of 0.1°C in water temperature change for a 30 cm deep water column during a 30 min time period results in an error of about 70 W m⁻² in stored heat energy flux. This stored heat energy error can be substantial, considering mean 30 min net radiation ranged from -50 to 500 W m⁻² within the Everglades wetland areas. Negative values of net radiation were common during the night, when incoming short-wave solar radiation was zero. The regression-defined parameter values served to minimize the error in water temperature changes computed with the convolution integral, and provided further insight regarding the variability of heat exchange processes acting within the wetland system.

[21] Regression minimized the objective function, $S(b)$, [Hill, 1998] that was quantitatively defined as

$$S(b) = \sum_{i=1}^{nt} \left(\Delta T_{w_i} - \Delta T'_{w_i}(b) \right)^2 \quad (10)$$

where b is a vector containing values of each of the parameters being regression estimated, nt is the number of water temperature changes measured in the field, ΔT_{w_i} is the i th measured water temperature change, $\Delta T'_{w_i}(b)$ is the equivalent of the i th measured water temperature change computed by the convolution integral (a function of b). Measured water temperature changes, ΔT_{w_i} , in $S(b)$ were derived from the German [2000] data as follows. Thirty minute mean water temperatures measured at the top and base of the water column were averaged to estimate the mean 30 min and vertical water column temperatures. The difference between two consecutive mean vertical water column temperatures was used as the mean vertical water column temperature change (ΔT_{w_i}).

[22] Field data requirements for equation (9) included time series of air temperature changes (ΔT_a) and water depths (D). These time series data were taken from the German [2000] data set. Field data were not available for the thermal exchange (k_{ex}) and alpha (α) coefficients, therefore these coefficients were estimated with regression to minimize equation (10). A conservative overestimate of the surface water's thermal memory also was used in order to solve equation (9) because it prevented errors in convolution-computed water temperature changes caused by truncation of the transfer function. For example, using 0.25 days

for the surface water's thermal memory truncates relatively large values of the transfer function (Figure 6). This truncation creates errors in convolution-computed water temperature changes (equation (9)) because air temperature changes occurring prior to 0.25 days are not multiplied by the transfer function and summed to compute the current water temperature changes. In contrast, over estimating the surface water's thermal memory only truncates very small values of the transfer function (Figure 6) which minimizes truncation errors. Thus a period of 12 days was used as a conservative overestimate of the surface water's thermal memory, based on the decay of the transfer function (Figure 6) for values of k_{ex} and D expected in this study. This 12 day thermal memory was used at all sites every year.

[23] The regression process was initiated by perturbing k_{ex} and α by 1% from their initial values to compute parameter sensitivities. These sensitivities were used to solve for estimates of k_{ex} and α that minimized $S(b)$. The detailed forms of $S(b)$, sensitivity, and regression equations are presented by Poeter and Hill [1998] and thus are not repeated here. $S(b)$ was considered minimized when the difference between two successive solutions for k_{ex} and α was less than the parameter tolerance criteria (equal to 0.01). Within this parameter tolerance, further regression iterations did not substantially reduce errors between changes in mean vertical water temperature computed with the convolution integral and those measured in the field.

3. Results

[24] The Florida Everglades, or "river of grass" [Douglas, 1947], is characterized by its low topographic relief; a broad array of aquatic, semiaquatic and upland habitats; and extensive wetland areas that include saw grass, cat tails, cypress strands, and tree islands (Figure 1). Evolution of the Everglades landscape, including natural processes, consequences of urbanization and water management activities, has been discussed extensively in many publications [Douglas, 1947; Parker et al., 1955; Renken et al., 2005] and therefore is not repeated here. It is reasonable to expect that Everglades wetland areas may store or release considerable amounts of heat energy, mostly because of the relatively large heat capacity of surface water and the extensive wetland areas covered by a column of surface water.

3.1. Surface Energy Budget

[25] A closer examination of terms in the surface energy budget for the study area (Figure 1) is discussed in this section. German [2000] reported that the mean annual magnitude of net radiation (R_n) ranged from 121 to 134 W m⁻² at nine sites in the Everglades wetland areas. Subdaily mean values of R_n were less than zero during the evening and night when long-wave radiation emitted from the vegetation, land, and surface water generally exceeded incoming atmosphere radiation. The magnitude of 30 min mean R_n was relatively large during the day, sometimes exceeding 500 W/m² when the intensity of incoming solar radiation was greatest.

[26] Energy is stored in the ecosystem biomass, specifically, in vegetation (G_{veg}), and in subsurface geologic media. When present, surface water generally is the primary medium for energy storage [Bidlake et al., 1996], largely because of its relatively high heat capacity, which is about

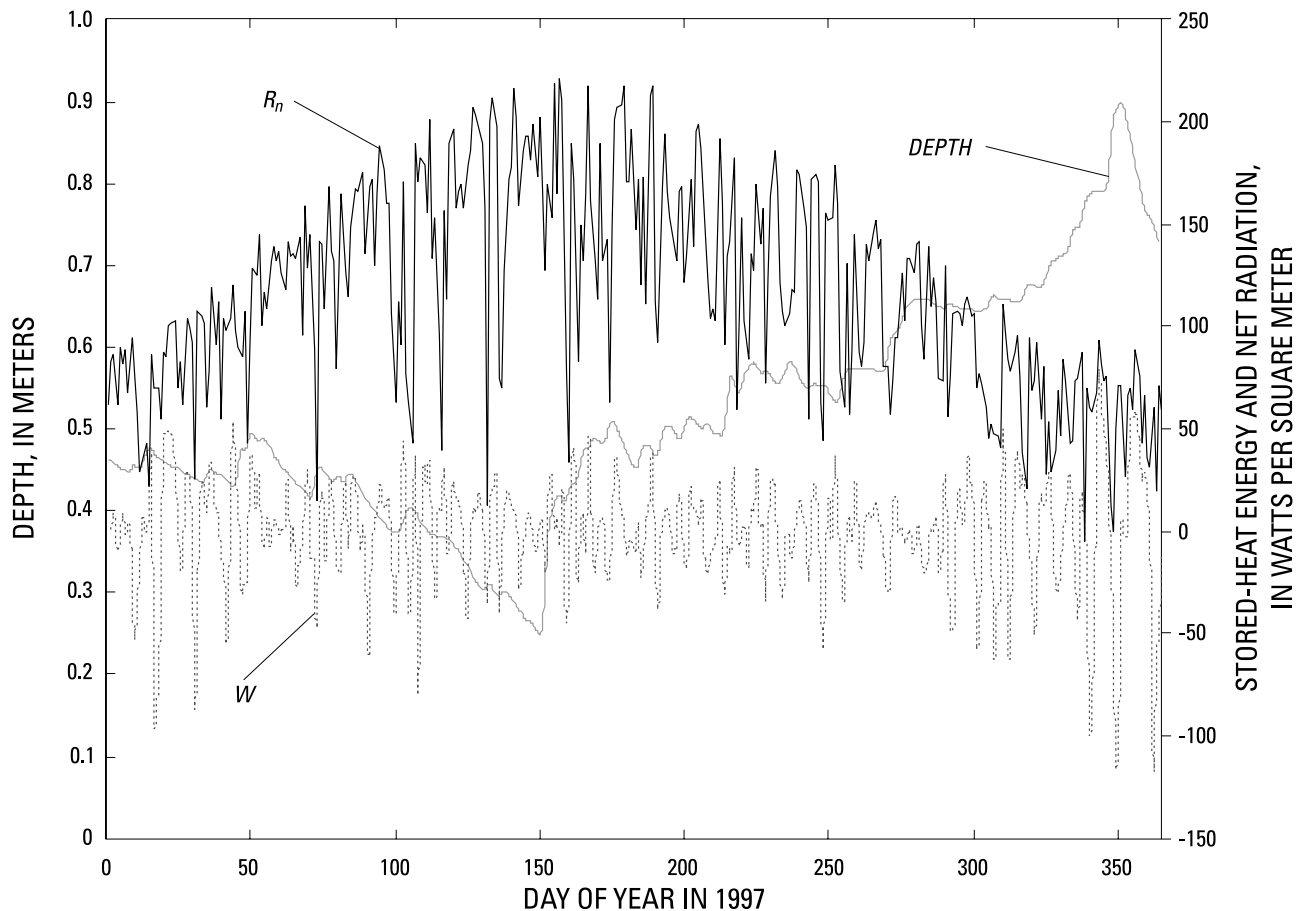


Figure 7. Net daily fluxes of stored heat energy (W), mean daily net radiation (R_n), and mean daily wetland water depth (DEPTH) at site 3 in 1997.

double the heat capacity of vegetation, soil minerals, and soil organic matter [Brutsaert, 1982]. Vegetation is rarely dense enough to create a large reservoir for energy. For example, vegetation density was measured at several locations along five transects in the Everglades wetland areas [Childers *et al.*, 2003]. The maximum vegetation density was about 4100 g/m^2 (dry weight). Assuming plant matter is 90% water, the equivalent surface-water depth of the maximum plant density was about 4 cm. This depth is minimal when considering water depths in the Everglades wetland areas can exceed 1 m.

[27] A component of the available energy for evapotranspiration not included in the surface energy budget (equation (1)), is the energy that is added to, or removed from, the wetlands through rainfall. An analysis of data [German, 2000] in the Everglades suggested energy fluxes attributed to rainfall can be considerable in hourly surface energy budgets; however, rainfall energy fluxes are relatively small compared to mean daily fluxes of net radiation. From 1996 to 2000, rainfall data were collected at sites 4 to 9 (Figure 1), and the energy flux from rainfall events was computed as described by Bogan *et al.* [2003, equation (12)] assuming the rainfall temperature was equal to the dew point temperature. The maximum and minimum energy fluxes from rainfall at the sites were 10 and -40 W m^{-2} , respectively, over the 4 year period. A positive flux implies the rainfall is warmer than the wetland surface water, and increases the amount of heat

energy to the system. Conversely, a negative flux implies the rainfall is colder than the wetland surface water, and decreases the amount of heat energy within the system. Fluxes of 10 and -40 W m^{-2} could be considerable within hourly surface energy budgets during rainfall events when incoming solar radiation is dampened by cloud cover. More than 93% of the time, however, the magnitude of heat energy flux from rainfall was less than one twentieth the magnitude of the mean daily net radiation.

3.2. Magnitude of Stored Heat Energy

[28] A time series plot shows mean daily net radiation (R_n), mean surface water depth, and daily fluxes of stored heat energy in the wetland surface water (W) at site 3 in 1997 (Figure 7). Fluxes of stored heat energy (W) were computed as the product of ΔT_s , D and heat capacity divided by the number of seconds in one day. During the winter, net radiation was relatively low, and air temperature varied considerably (Figure 4), resulting in fluxes of heat energy stored in wetland surface water that approached and even exceeded 50 W m^{-2} (Figure 7). Stored heat energy sometimes exceeded the magnitude of net radiation and thus, in some instances, was the dominant component of the daily wetland surface energy budget, particularly during the winter when solar radiation was relatively low.

[29] To assess the importance of W in wetland surface energy budgets, an importance ratio (R_{imp}), defined as the

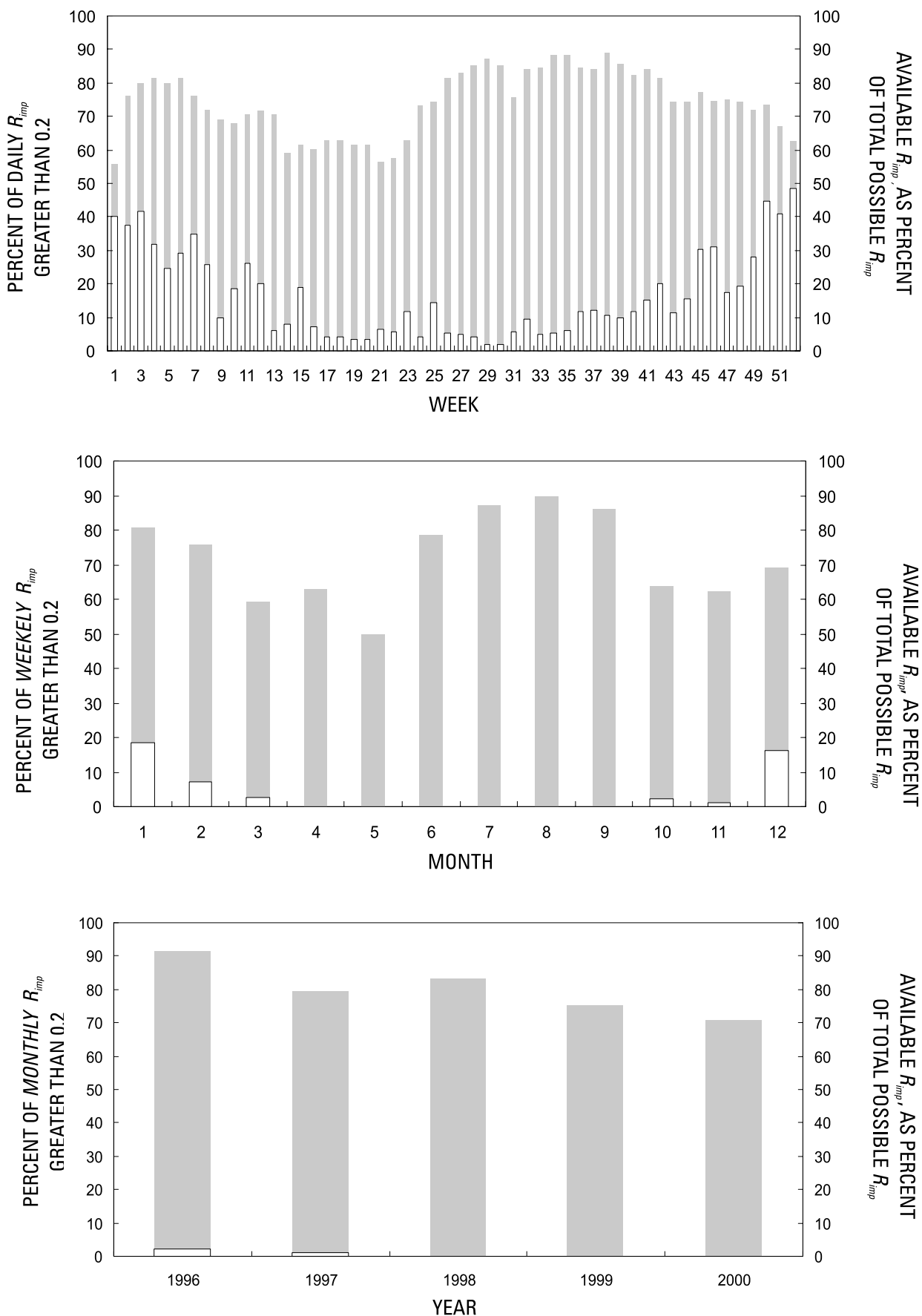


Figure 8. Percent of R_{imp} greater than 0.2 within a specified time period (white bars) and available R_{imp} expressed as a percent of the total possible R_{imp} (gray bars).

Table 2. Summary of Regression-Estimated Coefficients and Error Statistics for Comparison of 30 min Measured and Convolution Site Model Water Temperature Changes and Fluxes of Stored Heat Energy^a

Convolution Site Model	Regression-Defined Thermal Exchange Coefficient k_{ex} , $m\ s^{-1}$	Regression-Defined α	Number of Comparisons	Measured and Convolution Site Model-Computed Water Temperature Changes T		Measured and Convolution Site Model-Computed Fluxes of Stored Heat Energy W	
				R^2 of the Comparison	Mean Absolute Error of the Comparison, $^{\circ}C$	R^2 of the Comparison	Mean Absolute Error of the Comparison, $W\ m^{-2}$
S2_96	5.46	0.36	4,849	0.56	0.08	0.56	134.71
S2_97	5.94	0.46	6,050	0.60	0.09	0.56	154.25
S3_96	4.31	0.55	8,137	0.65	0.09	0.65	108.32
S3_97	3.88	0.57	8,089	0.65	0.08	0.63	95.90
S4_96	0.48	0.51	7,080	0.64	0.10	0.57	46.45
S4_97	1.53	0.33	4,585	0.57	0.09	0.47	50.56
S4_98	3.17	0.23	6,396	0.45	0.06	0.40	68.14
S4_99	0.45	0.73	2,578	0.70	0.12	0.69	35.40
S5_96	0.83	0.43	8,136	0.68	0.08	0.66	50.34
S5_97	0.85	0.44	5,042	0.75	0.08	0.69	31.60
S7_96	1.53	0.74	8,137	0.71	0.07	0.72	73.35
S7_97	1.46	0.71	7,469	0.68	0.09	0.65	61.58
S7_98	1.71	0.74	8,089	0.64	0.07	0.65	71.51
S7_99	1.85	0.65	7,915	0.70	0.08	0.70	77.46
S7_00	2.09	0.60	5,208	0.61	0.09	0.60	109.18
S8_97	1.50	0.54	1,079	0.54	0.14	0.67	27.90
S8_98	0.88	0.91	5,671	0.68	0.16	0.69	28.01
S8_99	1.33	0.83	2,706	0.73	0.11	0.72	39.38
S8_00	1.06	0.87	2,212	0.73	0.16	0.73	37.39
S9_98	0.11	0.94	1,287	0.70	0.06	0.65	8.99

^aSite locations are shown in Figure 1.

ratio of the absolute value of W to net radiation, was computed (Figure 8). The (1) heat capacity of water, (2) net change in mean vertical water column temperature from the beginning to the end of the time period of interest, and (3) mean surface water depth within the time period of interest were used to compute W for R_{imp} . For example, if daily R_{imp} were desired, W was computed as the product of the heat capacity of water, net change in mean vertical water column temperature from the beginning of the day to the end of the day, and the mean daily depth of surface water divided by the number of seconds in a day. In this daily case, R_{imp} was computed as the absolute ratio of mean daily net radiation and W . If a weekly R_{imp} was desired W was computed as the product of the heat capacity of water, net change in mean vertical water column temperature from the beginning of the week to the end of the week, and the weekly mean depth of the surface water divided by the number of seconds in a week. In this weekly case, R_{imp} values were computed as the absolute ratio of mean weekly net radiation to W .

[30] The percentage of time R_{imp} values were equal to or greater than a filter threshold of 0.2 (Figure 8) highlights time periods when W was a considerable part of the wetland surface energy budget. Also computed were the data availability of R_{imp} , expressed as the percentage of time sufficient data were available to compute R_{imp} . Data availability trends for R_{imp} were independent of the filter threshold trends for R_{imp} , which demonstrates the filter threshold trends are not an artifact of missing data.

[31] During week 1 (1–7 January) of years 1996–2000, about 40% of the daily R_{imp} values were equal to or greater than 0.2 at sites 2 to 5 and 7 to 9. A total of 105 daily R_{imp} values were calculated during week 1, of which 42 were

equal to or greater than the filter threshold value. During week 29 (early July), however, less than 5% of the daily R_{imp} values were equal to or greater 0.2. Although 165 daily R_{imp} values were calculated during this period, only 3 ratios were equal to or greater than the filter threshold value. This analysis suggests that W is more often a considerable component of the mean daily surface energy budget during the winter than the summer.

[32] As expected, temporal upscaling reduces the importance of changes in heat energy stored in wetland surface water in the surface energy budget. This assertion is supported by comparing the percentages of the R_{imp} values that exceed 0.2 over different time scales (Figure 8). For example, during week 1 (1–7 January) of years 1996–2000, about 40% of the daily R_{imp} were equal to or greater than the 0.2 filter threshold; however, during the entire month of January, less than 20% of the monthly total number of weekly R_{imp} were equal to or greater than the same filter threshold. This result is not surprising considering fluxes of stored heat energy in wetland surface water are inversely proportional to time, such that longer time periods result in smaller fluxes of stored heat energy.

3.3. Convolution Site Models

[33] Parameter estimation was applied to the discrete form of the convolution integral (equation (9)) and transfer function at 30 min time steps at sites 2 to 5 and 7 to 9 (Figure 1) for the 1996–2000 period. Each site/year combination defines a convolution site model. A total of 20 convolution site models were constructed (Table 2). The naming convention used for the site models is SN_XX, where N represents the site number (Figure 1) and XX represents the year. Graphical comparisons (Figures 9, 10,

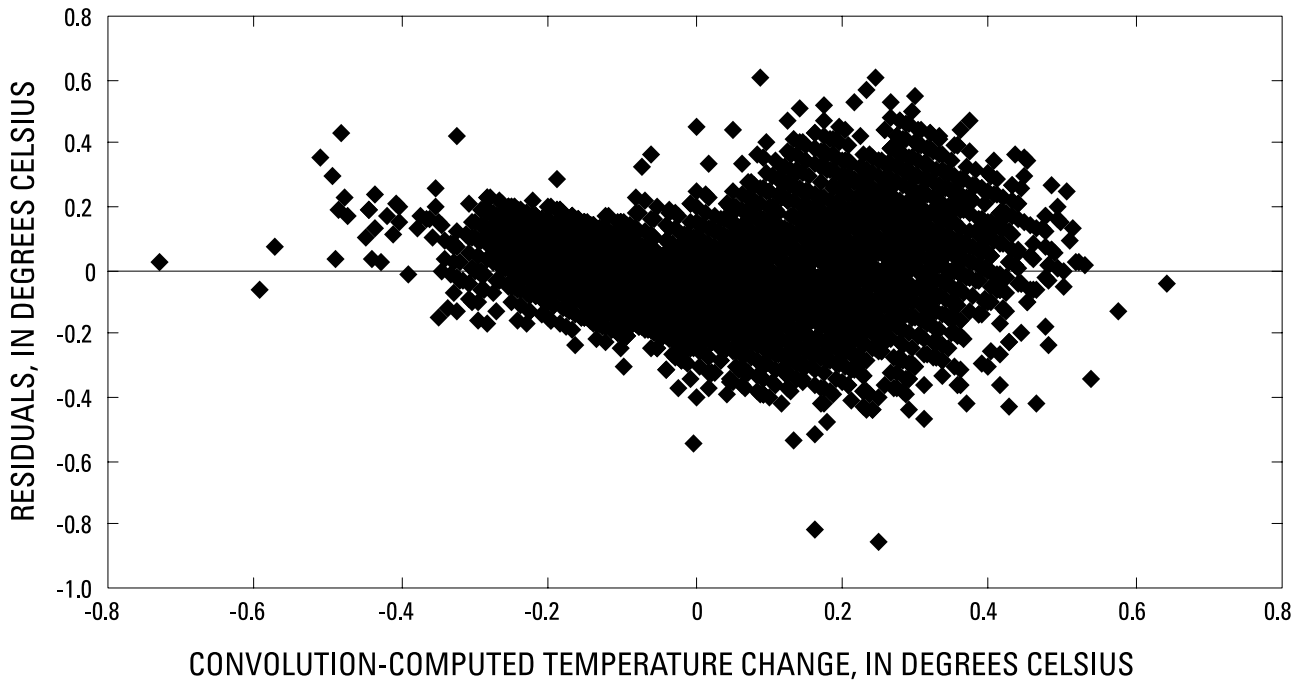


Figure 9. Comparison of 1996 residuals from measured values and convolution-computed mean vertical water temperature changes from site 3. Site location is shown in Figure 1.

11, and 12) of convolution computed water temperature changes and fluxes of stored heat energy versus residuals from measured values are presented for models with roughly average error statistics.

[34] Site 1 (not shown in the figures and tables) was not considered for analysis because of concerns that water temperature mostly was a function of water management activities, rather than natural changes in air temperature. Site 1 is located south of agricultural areas surrounding U.S.

Highway 98 (Figure 1). During the rainy season when water levels were high in the agricultural areas, surface water pumps conveyed water southward toward the Water Conservations Areas and impacted water temperatures measured at site 1. Site 6 (also not shown in the figures and tables) was similarly removed from consideration because air temperatures were recorded only to 1°C precision, resulting in relatively large error statistics for the convolution site models. Because stored heat energy changes in wetland

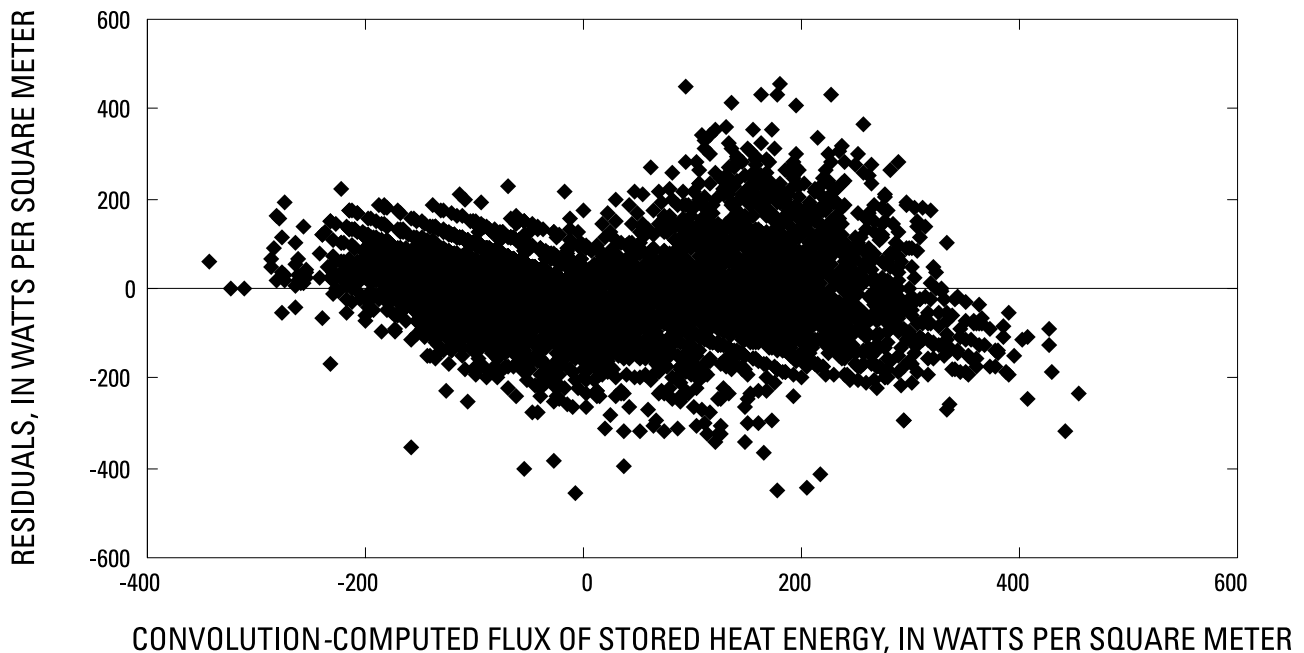


Figure 10. Comparison of 1996 residuals from measured fluxes of stored heat energy and convolution computed fluxes of stored heat energy from site 3. Site location is shown in Figure 1.

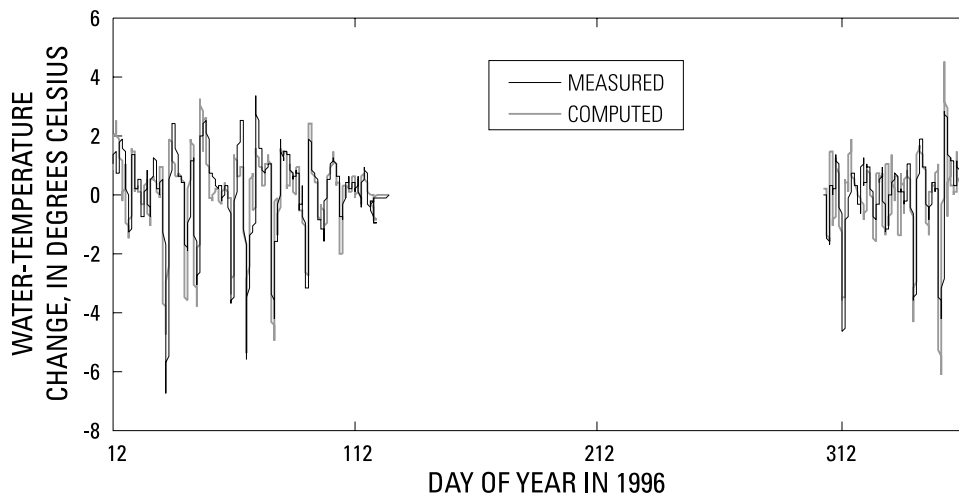


Figure 11. Measured and convoluted-computed net daily water temperature changes from site 3. Site location is shown in Figure 1. Missing data indicate that analysis was not performed for the period.

surface water are more often a considerable component of the surface energy budget during winter (Figures 7 and 8), all convolution site models included only the November to April winter season. During the summer, net radiation dominates the surface energy budget because of the magnitude of solar radiation, and therefore the need for accurate estimates of stored heat energy changes in wetland surface water is less critical.

[35] In general, the convolution site models performed adequately in computing 30 min mean vertical water column temperature changes during winter (Table 2). The R^2 values for computed and measured water temperature changes ranged from 0.45 to 0.75, with an average of 0.65. The mean absolute error for the comparison ranged from 0.06 to 0.16°C, with an average of 0.10°C. A graphical comparison of 1996 convolution computed water temperature changes versus the residuals from field-measured water temperature changes at site 3 (Figure 9) indicates that declines in water temperature are more precisely computed than increases in water temperature. This bias was present within each convolution site model (Table 2) based on visual inspection of computed versus residual plots. Al-

though a mechanism for this bias is unclear, its consequence is that in general during the winter releases of heat energy from surface water storage ($-W$) will be more accurately computed by the convolution sites models than fluxes of heat energy into surface water storage ($+W$).

[36] The water temperature changes computed from the convolution site models also seem to work well for approximating 30 min fluxes of stored heat energy in wetland surface water in the Everglades (Table 2). Fluxes of stored heat energy in wetland surface water were approximated as the product of ΔT_w (computed by the convolution site models), D , and heat capacity divided by the number of seconds in 30 min and compared to the fluxes of stored heat energy computed with field-measured changes in mean vertical water column temperature. The R^2 values determined for the comparison ranged from 0.40 to 0.73, with an average of 0.63. The mean absolute error for the comparison ranged from about 8.99 to 154.25 $W m^{-2}$, with an average of 65.52 $W m^{-2}$. A graphical comparison of 1996 convolution-computed fluxes of stored heat energy versus residuals from field-measured fluxes of stored heat energy at site 3 (Figure 10) indicates bias similar to that in Figure 9

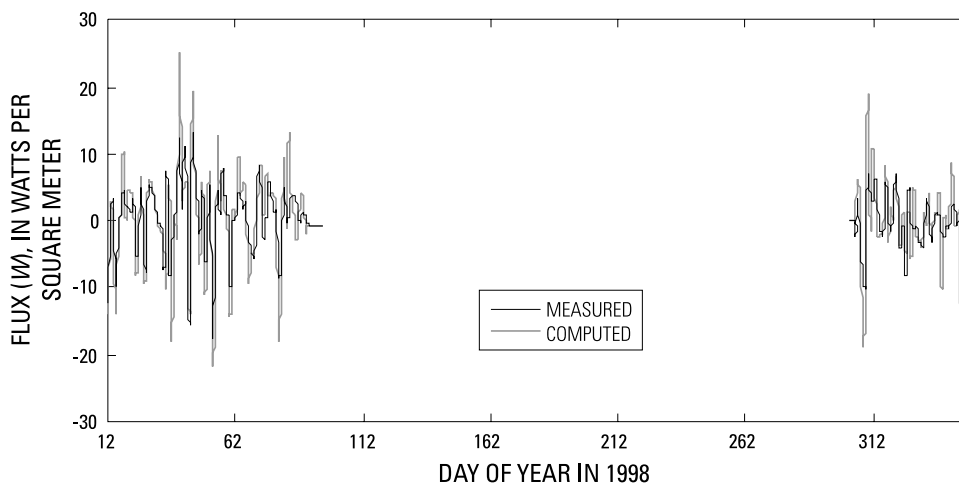


Figure 12. Measured and convoluted-computed net daily fluxes of stored heat energy (W) from site 3. Site location is shown in Figure 1. Missing data indicate that analysis was not performed for the period.

Table 3. Summary of Error Statistics for Comparison of Measured and Convolution-Computed Net Daily Water Temperature Changes and Fluxes of Stored Heat Energy^a

Convolution Site Model	Measured and Computed Net Daily Water Temperature Changes dT		Measured and Computed Net Daily Fluxes of Stored Heat Energy W	
	R ² of the Comparison	Mean Absolute Error of the Comparison, °C	R ² of the Comparison	Mean Absolute Error of the Comparison, W m ⁻²
S2_96	0.46	0.58	0.45	22.24
S2_97	0.63	0.50	0.60	19.94
S3_96	0.66	0.64	0.64	16.40
S3_97	0.57	0.68	0.56	17.99
S4_96	0.84	0.52	0.82	2.35
S4_97	0.72	0.78	0.64	7.93
S4_98	0.50	0.42	0.49	9.50
S4_99	0.85	0.54	0.85	2.47
S5_96	0.70	0.53	0.69	4.15
S5_97	0.74	0.58	0.75	5.19
S7_96	0.73	0.62	0.72	12.51
S7_97	0.72	0.57	0.69	9.20
S7_98	0.79	0.64	0.78	15.94
S7_99	0.59	0.49	0.61	11.87
S7_00	0.64	0.52	0.62	9.84
S8_97	0.78	0.73	0.78	3.07
S8_98	0.72	1.00	0.62	3.64
S8_99	0.57	0.79	0.70	6.97
S8_00	0.80	1.04	0.76	4.65
S9_98	0.75	0.62	0.57	1.28

^aSite locations are shown in Figure 1.

because heat content is derived from water temperature changes. As a consequence, each convolution site model computes fluxes of heat energy leaving surface water storage more precisely than fluxes of energy into surface water storage.

[37] The site convolution models yielded reasonable estimates of net daily changes in both wetland surface water temperature and fluxes of stored heat energy during winter months (Table 3). Net daily water temperature changes were estimated as the daily sum of water temperature changes that occurred during 30 min increments. The R² values between measured and computed net daily water temperature changes ranged from 0.46 to 0.85, with an average of 0.69. The mean absolute error for the comparison ranged from 0.42 to 1.04, with an average of 0.64°C. A graphical comparison of measured and convolution-computed net daily water temperature changes at site 3 in 1996 is shown (Figure 11). For computing net daily fluxes of stored heat energy, R² statistics for the convolution site models ranged from 0.45 to 0.85, with an average of 0.67. The mean absolute error for the comparison ranged from 1.28 to 22.24 W m⁻², with an average of 9.36 W m⁻². A graphical comparison of measured and convolution-computed net daily fluxes of stored heat energy at site 8 in 1998 is shown in Figure 12.

4. Discussion

[38] The convolution site models and methods used to determine when and where changes in stored heat energy

were a considerable component of the surface energy budget revealed some results worthy of discussion. These results include (1) nighttime “inversions” of the wetland water column due to thermal convective mixing, (2) variability in regression-defined k_{ex} and α coefficients, (3) data requirements and transfer value of the convolution models to locations other than the Everglades wetlands areas, and (4) the relative accuracy of the convolution models compared to simpler approaches for approximating wetland surface water temperature changes, and ultimately, fluxes of stored heat energy.

[39] In Everglades wetland areas, thermal stratification in the surface water column was common during the day, with near-surface water temperatures rising more than water temperatures at depth (Jenter et al., U.S. Geological Survey, written communication, 2003). During the evening, the water column was thermally mixed by a surface water inversion process (convective mixing). Mixing occurred when nighttime air temperatures caused cooling of a thin layer at the top of the surface water, creating a negatively buoyant boundary from which surface water “fingered” downward to the bottom of the water column. This process is noteworthy because field-measured water temperature changes used in S(b) were affected by this thermal stratification and convective mixing. Because regression was used to minimize S(b), regression-defined values of k_{ex} and α likely account for some of the temperature variability caused by this inversion process.

[40] Spatial variability in the regression-defined k_{ex} coefficients provided some insight into the heat exchange processes acting on a wetland system. Regression-defined estimates of k_{ex} ranged from 0.11 m s⁻¹ at site 9 in 1998 to 5.94 m s⁻¹ at site 2 in 1997 (Table 2) and a statistically significant difference existed between open water and vegetated sites. Statistically significant difference was established using the nonparametric Kruskal-Wallis rank-sum test. This rank-sum test exceeded the critical value for chi-square at the significance level of 0.01 with one degree of freedom, suggesting the null hypothesis of equal distributions could be rejected and a statistically significant difference existed for k_{ex} between open water and vegetated sites. Several mechanisms may explain larger k_{ex} values over open water sites, including enhanced wind-driven and thermal convective mixing. Wind-driven mixing would be greater over open water sites because vegetational surfaces, such as plant leaves, stalks, and stems are not present to provide roughness obstacles. Likewise, thermal convective mixing would be greater over open water sites because vegetational surfaces are not present to increase frictional resistance to vertical surface water flow and reduce convective and radiative energy transport through the air-water interface. Increased mixing (either wind-driven or thermal convective) would homogenize the entire water column relatively quickly until the water temperature approximately equaled the air temperature. In contrast, decreased mixing in vegetated sites would homogenize the water column more slowly.

[41] Spatial variability in the regression-defined α coefficients also was present, although not statistically significant, in the Everglades wetland areas. Alpha (α) coefficients ranged from 0.23 at site 4 to 0.94 at site 9 in 1998, with an average of about 0.5 and 0.6 for open water and vegetated

Table 4. Comparison of Error Statistics for Different Methods of Computing Water Temperature Changes and Fluxes of Stored Heat Energy at an Open Water Site (Site 3) and a Dense Saw Grass Site (Site 4) for 30 min and Daily Time Steps in 1996^a

Method	Time Step	R ² Coefficient	Mean Absolute Error
<i>Site 3 (Open Water)</i>			
1	30 min	0.65	0.09
2	30 min	0.27	0.15
3	30 min	0.27	0.29
4	daily	0.66	16.14
5	daily	0.64	15.68
6	daily	0.44	21.19
7	daily	0.66	29.09
<i>Site 4 (Dense Saw Grass)</i>			
1	30 min	0.64	0.10
2	30 min	0.03	0.07
3	30 min	0.03	0.30
4	daily	0.82	2.35
5	daily	0.52	3.31
6	daily	0.45	4.71
7	daily	0.52	6.41

^aLocations of sites 3 and 4 are shown in Figure 1. The MAE values are in degrees Celsius for the 30 min time steps and in watts per square meter for the daily time steps. Method: 1, convolution approach; 2, expressing water temperature changes as a simple regression-defined function of air temperature changes; 3, setting water temperature changes equal to air temperature changes; 4, daily compositing of the convolution model results; 5, expressing net daily water temperature changes as a simple regression-defined function of net daily air temperature changes; 6, daily compositing of the results of expressing 30 min water temperature changes as a simple regression-defined function of air temperature changes; 7, setting net daily water temperature changes equal to net daily air temperature changes.

sites, respectively (Table 2). Statistically significant difference between open water and vegetated sites also was examined using the nonparametric Kruskal-Wallis rank-sum test. This rank-sum test was less than the critical value for chi-square at the significance level of 0.01 with one degree of freedom, suggesting the null hypothesis of equal distributions could not be rejected and no statistically significant difference exists for α between open water and vegetated sites.

[42] The ability of the convolution site models to compute water temperature changes and fluxes of stored heat energy at other locations depends on the area of interest. The convolution models and regression-defined k_{ex} and α coefficients are more directly transferable in the winter to similar humid subtropical wetland areas, suggesting that the only data requirements in these areas are air temperature and wetland water column depth. The convolution models also may be applied in the winter over lakes or other land masses associated with a sluggish surface water drainage including coastal bays, mangrove or cypress swamps, and estuaries. The transfer value of this analysis, however, diminishes at locations with vegetation other than saw grass, cattails, rush, and open water wetlands because the regression-defined k_{ex} and α coefficients (Table 2) may not apply. New regression experiments may be required to define values for k_{ex} and α that are specific to the land cover of interest. This more complicated case requires time series data for water temperature in addition to time series data for air temperature and surface water depth.

[43] Considering the modest mathematical complexity of the convolution approach, an obvious question is: Do

simpler methods exist with comparable or improved error statistics for computing 30 min and net daily changes in surface water temperature, and ultimately, fluxes of stored heat energy? Seven methods were evaluated at an open water site (site 3) and a dense saw grass site (site 4) for 30 min and daily time steps in 1996 (Table 4). These methods include, for the 30 min time step, (1) the convolution approach, (2) expressing water temperature changes as a simple regression-defined function of air temperature changes, and (3) setting water temperature changes equal to air temperature changes, and for the daily time step, (1) daily composites of the convolution results, (2) expressing net daily water temperature changes as a simple regression-defined function of net daily air temperature changes, (3) daily composites of the results of expressing 30 min water temperature changes as a simple regression-defined function of air temperature changes, and (4) setting net daily water temperature changes equal to net daily air temperature changes.

[44] For the 30 min time steps at the open water site (site 3), the convolution approach (method 1) clearly outperforms the simpler approaches (methods 2 and 3) for computing changes in the mean vertical water column temperature (Table 4). With method 1, the R² values were 0.65 and the mean absolute error was 0.09°C at site 3. A simpler approach, that is, setting the mean vertical water column temperature change equal to the air temperature change (method 3), produced the largest error statistics. With method 3, the R² values were 0.27 and the mean absolute error was 0.29°C at site 3. The results likely are similar for fluxes of stored heat energy because heat content is derived from water temperature changes.

[45] For the 30 min time steps at the dense saw grass site (site 4), the convolution approach (method 1) outperforms the simpler approaches (methods 2 and 3) for computing changes in the mean vertical water column temperature (Table 4). With method 1, the R² values were 0.64 and the mean absolute error was 0.10°C. Although the simpler method 2 produced a smaller mean absolute error (equal to 0.07°C) than method 1, the results for method 2 were almost completely uncorrelated (R² equal to 0.03) to measured mean vertical water temperature changes.

[46] For daily time step at the open water site 3, there may be simpler methods than daily compositing the site convolution model results for computing water temperature changes, and ultimately fluxes of stored heat energy, with comparable error statistics. For example, at site 3 in 1996, expressing daily mean water column temperature changes as a regression-defined function of net daily air temperature changes (method 5) produced a slightly lower R² (equal to 0.64 for method 5 versus 0.66 for method 4), and a slightly lower mean absolute error (equal to 15.69 W m⁻² for method 5 versus 16.14 W m⁻² for method 4). The regression relation for site 3 was $\frac{\Delta T_w}{\Delta t} = \chi_1 \Delta T_a + \chi_2$, with χ_1 and χ_2 equal to 0.027 and 0.475, respectively.

[47] For daily time steps at the dense saw grass site 4, daily compositing the site convolution model approach (method 4) also clearly outperformed the simpler approaches (methods 5–7) for computing net daily fluxes of stored heat energy (Table 4). With method 4, the R² value was 0.82, and the mean absolute error was 2.35 W m⁻² at site 4. For the simpler approaches (methods 5–7), the R² values ranged from 0.45 (method 6) to 0.52 (methods 5 and

7), and the mean absolute errors ranged from 3.31 (method 5) to 6.41 W m^{-2} (method 7).

5. Limitations

[48] Several limitations are apparent in this study. Certain spatial and temporal characteristics limit the accuracy of results when the convolution integral is applied to compute fluxes of stored heat energy. Also, the use of water temperature at only two depths to derive a mean vertical water column temperature change is questionable. Finally, the bias in computing water temperature changes with the convolution integral is problematic.

[49] Spatial and temporal characteristics limit the accuracy of results when the convolution integral is applied to compute fluxes of stored heat energy. Spatially, the results are more accurate at sites where water temperature changes are mostly controlled by air temperature changes. Although air temperature changes explain most of the variability in water temperature changes (Figure 4), other heat exchange processes also impact water temperature, including water management activities (site 1), evaporative cooling, rainfall, and perhaps surface water and groundwater interactions. Temporally, accuracy increases at daily time steps at all sites (Tables 2 and 3), because the errors at 30 min time steps are mostly normally distributed with a zero mean and unbiased. If the 30 min errors were nonnormal and highly biased, errors statistics at daily time steps likely would increase.

[50] The use of water temperature at only two depths to derive a mean vertical water column temperature change is questionable. Data availability necessitated this approach for sites 2 to 5 and 7 to 9. At other sites, water temperature was measured vertically every 10 cm [Schaffranek and Riscassi, 2004] at 30 min intervals. Changes in the mean vertical water column temperature were computed from August of 2000 through March 2001 using (1) the high-frequency data, and (2) assuming only the top and bottom water column temperatures were available. The mean absolute error between these two alternatives was about 0.3°C . This translates into an difference of greater than 300 W m^{-2} at 30 min time steps assuming the water column is 50 cm deep. The water temperature changes measured with the high-resolution data may be more reliable. Thus, if reliable data are available, it seems prudent to compute fluxes of stored heat energy with high vertical resolution measurements of surface water temperature. When reliable data are not available, air temperature changes can be applied to the convolution integral as outlined in this paper to estimate fluxes of stored heat energy.

[51] The bias in computing water temperature changes also is problematic. The convolution site models compute a decrease in water temperature more precisely than an increase in water temperature at 30 min time steps. If the underlying mechanism for the bias could be resolved, the R^2 values and standard errors for water temperature change and fluxes of stored heat energy (Tables 2 and 3) likely would improve.

6. Conclusions

[52] On the basis of the results from this study, several conclusions can be drawn regarding wetland surface energy

budgets and estimation of changes in heat energy stored in a column of wetland surface water. These conclusions likely are directly transferable to other humid subtropical wetlands dominated by open water, saw grass and rush vegetation communities.

[53] 1. Changes in heat energy stored in wetland surface water were a substantial component of the surface energy budget more frequently in the winter than in the summer. This result is explained by the magnitude of solar radiation during the winter and the control of air temperature on water temperature. Specifically, solar radiation during the winter was relatively low and air temperature changes were more variable, creating water temperature changes that were more variable. Interaction of these two factors resulted in fluxes of stored heat energy in wetland surface water that approached the magnitude of net radiation more frequently during the winter than in the summer.

[54] 2. The magnitude of changes in heat energy stored in wetland surface water generally decreased as surface energy budgets were upscaled temporally. Daily fluxes of stored heat energy accounted for 20% or more of the magnitude of mean daily net radiation for about 40% of the data examined here. Weekly fluxes of stored heat energy were 20% or more of the magnitude of mean weekly net radiation for about 20% of the same data examined here. This result is explained by fluxes of stored heat energy being inversely proportional to time, such that larger lengths of time result in smaller fluxes of stored heat energy.

[55] 3. Air temperature changes can be used to approximate changes in water temperature and, ultimately, fluxes of stored heat energy in wetland surface water through the application of a convolution integral with a regression-defined transfer function. This method was most accurate at sites where surface water temperature changes mostly were controlled by air temperature changes rather than water management activities, evaporative cooling or other heat exchange processes. The accuracy of computed fluxes of stored heat energy also increased when 30 min convolution results were composited to net daily values.

[56] 4. Heat energy exchanges more rapidly at the air-water interface over open water sites than at vegetated sites, as suggested by a statistically significant difference between the values of regression-defined thermal exchange coefficients at open water and vegetated sites. Several mechanisms may explain this difference, including enhanced wind-driven and thermal convective mixing at open water sites due to less vegetational surfaces providing roughness obstacles.

[57] 5. Energy fluxes from rainfall generally were minimal compared to mean daily fluxes of net radiation, indicating that energy fluxes from rainfall probably do not need to be considered within surface energy budgets at daily and larger time scales.

[58] 6. Wetland vegetation was not dense enough to create a large equivalent surface water reservoir for energy. The equivalent surface water depth of the maximum vegetation density was about 4 cm. This depth was minimal considering water depths in the Everglades frequently exceeded 1 m, and suggests changes in heat energy stored in wetland vegetation likely can be ignored

with little error in surface energy budgets at daily and larger time scales.

Appendix A

[59] This appendix documents the solution of ordinary differential equation (4) to obtain equation (5) described in this paper. Equation (4) is expressed as

$$\frac{d(T_w^e - T_w)}{dt} = -k_{ex} \frac{(T_w^e - T_w)}{D}.$$

Rearrange and integrate equation (4) so that

$$\int \frac{1}{(T_w^e - T_w)} d(T_w^e - T_w) = \frac{-k_{ex}}{D} \int dt. \quad (\text{A1})$$

Let $x = (T_w^e - T_w)$ and then $dx = d(T_w^e - T_w)$. Substitute x and dx into equation (A1) where:

$$\int \frac{1}{x} dx = \frac{-k_{ex}}{D} \int dt, \quad (\text{A2})$$

which equals

$$\ln x = \frac{-k_{ex}}{D} t + C_1. \quad (\text{A3})$$

Take the exponent of both sides so that equation (A3) equals

$$x = C_2 e^{\frac{-k_{ex}}{D} t}; \quad (\text{A4})$$

note that C_2 equals e^{C_1} .

[60] Substitute back for x so that equation (A4) equals

$$T_w^e - T_w = C_2 e^{\frac{-k_{ex}}{D} t}. \quad (\text{A5})$$

If we solve equation (A5) at the initial condition of $t = 0$, then

$$T_w^e - T_w = C_2. \quad (\text{A6})$$

Introduce the assumption that a given air temperature change, ΔT_a [T], eventually causes an equivalent water temperature change, where the water temperature change is expressed as the difference between the equilibrium and actual water temperatures, thus

$$T_w^e - T_w = C_2 = \Delta T_a. \quad (\text{A7})$$

Substitute ΔT_a in equation (A5) so that

$$T_w^e - T_w = \Delta T_a e^{\frac{-k_{ex}}{D} t}. \quad (\text{A8})$$

By rearranging equation (A8), the formula becomes equation (5), which is

$$T_w = T_w^e - \Delta T_a e^{\frac{-k_{ex}}{D} t}.$$

[61] **Acknowledgments.** The U.S. Geological Survey (USGS) and South Florida Water Management District jointly funded this study. Eric Swain (USGS, Miami, Florida) helped derive equations. Mark Zucker (USGS, Miami, Florida) provided review comments and identified statistical methods appropriate for application in this study. Robert Renken (USGS, Miami, Florida), Amy Swancar (USGS, Tampa, Florida) and three anonymous Water Resources Research reviewers provided comments that improved the manuscript quality. Review comments from Water Resources Research Associate Editor Michiaki Sugita are gratefully acknowledged for substantially improving the manuscript quality.

References

- Abtew, W., and J. Obeysekera (1995), Lysimeter study of evapotranspiration of cattails and comparison of three estimation methods, *Trans. ASAE*, 38(1), 121–129.
- Anderson, M. C., J. M. Norman, G. R. Diak, W. P. Kustas, and J. R. Mecikalski (1997), A two-source time-integrated model for estimating surface fluxes using thermal infrared remote sensing, *Remote Sens. Environ.*, 60, 195–216.
- Bastiaanssen, W. G. M., M. Ahmad, and Y. Chemin (2002), Satellite surveillance of evaporative depletion across the Indus basin, *Water Resour. Res.*, 38(12), 1273, doi:10.1029/2001WR000386.
- Besbes, M., and G. DeMarsily (1984), From infiltration to recharge: Use of a parametric transfer function, *J. Hydrol.*, 74, 271–293.
- Bidlake, W. R., W. M. Woodham, and M. A. Lopez (1996), Evapotranspiration from areas of native vegetation in west-central Florida, *U.S. Geol. Surv. Water Supply Pap.*, 2430, 35 pp.
- Bogan, T., O. Mohseni, and H. G. Stefan (2003), Stream temperature–equilibrium temperature relationship, *Water Resour. Res.*, 39(9), 1245, doi:10.1029/2003WR002034.
- Bowen, I. S. (1926), The ratio of heat losses by conduction and by evaporation from any water surface, *Phys. Rev.*, 27(6), 779–787.
- Brutsaert, W. (1982), *Evaporation Into the Atmosphere: Theory, History, and Applications*, 299 pp., Springer, New York.
- Campbell, G. S., and J. M. Norman (1998), *An Introduction to Environmental Biophysics*, 281 pp., Springer, New York.
- Childers, D., et al. (2003), Decadal change in vegetation and soil phosphorus pattern across the Everglades landscape, *J. Environ. Qual.*, 32, 344–362.
- Dodge, J. C. I. (1959), A general theory of the unit hydrograph, *J. Geophys. Res.*, 64(2), 241–256.
- Douglas, M. S. (1947), *The Everglades: River of Grass*, Mockingbird Books, St. Simons Island, Ga.
- Edinger, J. E., D. W. Duttweiler, and J. C. Geyer (1968), The response of water temperatures to meteorological conditions, *Water Resour. Res.*, 4(5), 1137–1143.
- German, E. R. (2000), Regional evaluation of evapotranspiration in the Everglades, *U.S. Geol. Surv. Water Resour. Invest. Rep.*, 00-4217, 48 pp.
- Hill, M. C. (1998), Methods and guidelines for effective model calibration, *U.S. Geol. Surv. Water Resour. Invest. Rep.*, 98-4005, 90 pp.
- Islam, S., E. Eltahir, and L. Jiang (2002), Satellite-based evapotranspiration estimation, final report, 74 pp., South Fla. Water Manage. Dist., West Palm Beach.
- Jacobs, J. M., and S. R. Satti (2001), Evaluation of reference evapotranspiration methodologies and AFSIRS crop water use simulation model, report, 113 pp., St. Johns River Water Manage. Dist., Palatka, Fla.
- Lietz, A. C. (2000), Analysis of water-quality trends at two discharge stations—one within Big Cypress National Preserve and one near Biscayne Bay—southern Florida, 1966–94, *U.S. Geol. Surv. Water Resour. Invest. Rep.*, 00-4099, 35 pp.
- Liu, J., J. M. Chen, and J. Cihlar (2003), Mapping evapotranspiration based on remote sensing: An application to Canada's landmass, *Water Resour. Res.*, 39(7), 1189, doi:10.1029/2002WR001680.
- Long, A. J., and L. D. Putnam (2004), Linear model describing three components of flow in karst aquifers using ^{18}O data, *J. Hydrol.*, 296, 254–270.
- Lott, R. B., and R. J. Hunt (2001), Estimating evapotranspiration in natural and constructed wetlands, *Wetlands*, 21(4), 614–628.
- Mohseni, O., G. S. Heinz, and T. R. Erickson (1998), A nonlinear regression model for weekly stream temperatures, *Water Resour. Res.*, 34, 2685–2692.
- Monteith, J. L., and M. Unsworth (1990), *Principles of Environmental Physics*, 291 pp., Elsevier, New York.
- Morel-Seytoux, H. J. (1984), From excess infiltration to aquifer recharge: A derivation based on the theory of flow of water in unsaturated soils, *Water Resour. Res.*, 20, 1230–1240.

- Norman, J. M., M. C. Anderson, W. P. Kustas, A. N. French, J. Mecikalski, R. Torn, G. R. Diak, T. J. Schmugge, and B. C. W. Tanner (2003), Remote sensing of surface energy fluxes at 10¹-m pixel resolutions, *Water Resour. Res.*, 39(8), 1221, doi:10.1029/2002WR001775.
- O'Reilly, A. M. (2004), A method for simulating transient ground-water recharge in deep water-table settings in central Florida by using a simple water-balance/transfer-function model, *U.S. Geol. Surv. Sci. Invest. Rep.*, 2004-5195, 49 pp.
- Parker, G. G., et al. (1955), Water resources of southeastern Florida, with special reference to the geology and ground water of the Miami area, *U.S. Geol. Surv. Water Supply Pap.*, 1255, 965 pp.
- Penman, H. L. (1948), Natural evaporation from open water, bare soil, and grass, *Proc. R. Soc. London, Ser. A*, 193, 120–146.
- Poeter, E. P., and M. C. Hill (1998), Documentation of UCODE: A computer code for universal inverse modeling, *U.S. Geol. Surv. Water Resour. Invest. Rep.*, 98-4080, 116 pp.
- Priestley, C. H. B., and R. J. Taylor (1972), On the assessment of surface heat flux and evaporation using large scale parameters, *Mon. Weather Rev.*, 100, 81–92.
- Renken, R. A., et al. (2005), Impact of anthropogenic development on coastal ground-water hydrology in southeastern Florida, 1900–2000, *U.S. Geol. Surv. Circ.*, 1275, 77 pp.
- Schaffranek, R. W., and A. L. Riscassi (2004), Flow velocity, water temperature, and conductivity at selected locations in Shark River slough, Everglades National Park, Florida: July 1999–August 2001, *U.S. Geol. Surv. Open File Rep.*, 02-159, 40 pp.
- Small, E. E., and S. A. Kurc (2003), Tight coupling between soil moisture and the surface radiation budget in semiarid environments: Implications for land-atmosphere interactions, *Water Resour. Res.*, 39(10), 1278, doi:10.1029/2002WR001297.
- Sumner, D. M. (2001), Evapotranspiration from a cypress and pine forest subjected to natural fires in Volusia County, Florida, 1998–99, *U.S. Geol. Surv. Water Resour. Invest. Rep.*, 01-4245, 56 pp.
- Weiler, M., B. L. McGlynn, K. J. McGuire, and J. J. McDonnell (2003), How does rainfall become runoff? A combined tracer and runoff transfer function approach, *Water Resour. Res.*, 39(11), 1315, doi:10.1029/2003WR002331.
- Wilson, K. B., et al. (2002), Energy partitioning between latent and sensible heat flux during the warm season at FLUXNET sites, *Water Resour. Res.*, 38(12), 1294, doi:10.1029/2001WR000989.
- Wu, J., R. Zhang, and J. Yang (1997), Estimating infiltration recharge using a response function model, *J. Hydrol.*, 198, 124–139.

A. Castillo and W. B. Shoemaker, Center for Water and Restoration Studies, Florida Integrated Science Center, U.S. Geological Survey, 9100 NW 36th Street, Suite 107, Miami, FL 33178, USA. (bshoemak@usgs.gov)

D. M. Sumner, Center for Aquatic Resource Studies, Florida Integrated Science Center, U.S. Geological Survey, 224 West Central Parkway, Suite 1006, Altamonte Springs, FL 32714, USA. (dmsumner@usgs.gov)